https://doi.org/10.20575/00000049
Polar Data Journal, Vol. 7, 58–71, August 2023

Spatiotemporally continuous temperature monitoring using optical fibers (Loop1) in the internal forest areas in Alaska for the period from 2015 to 2016

Kazuyuki SAITO [1,2]*, Go IWAHANA [2], Hiroki IKAWA[3], Hirohiko NAGANO[4], and Robert BUSEY [2]**

[1] Japan Agency for Marine-Earth Science and Technology (JAMSTEC), 3173-25 Showamachi, Kanazawaku, Yokohama, Kanagawa 236-0001.

[2] International Arctic Research Center, University of Alaska Fairbanks, 2160 Koyukuk Drive, Fairbanks, AK 99775-7340, USA.

[3] Hokkaido Agricultural Research Center, National Agriculture and Food Research Organization, 1 Hitsujigaoka, Toyohira, Sapporo, Hokkaido 062-8555.

[4] Institute of Science and Technology, Niigata University, 8050 Ikarashi 2-no-cho, Nishiku, Niigata, Niigata 950-2181.

**Current affiliation: Alaska-Pacific River Forecast Center, National Weather Service, National Oceanic and Atmospheric Administration,6930 Sand Lake Rd., Anchorage, AK 99502, USA.

*Corresponding author. Kazuyuki Saito (ksaito@jamstec.go.jp)

(Received February 2, 2023; Accepted July 14, 2023)

Abstract: A fiber-optic DTS (distributed temperature sensing) system using Raman-scattering optical time domain reflectometry was implemented at a research site in the interior of Alaska (Poker Flat Research Range) to delineate the spatiotemporal characteristics of the variations in air, surface, and ground temperatures associated with the boreal forest heterogeneity in terms of surface and canopy conditions. A fiber-optic cable sensor (multi-mode, GI50/125, dual-core; 3.4 mm) was deployed across the landscape that enables temperature measurements at high spatiotemporal resolution (0.5 m intervals at every 30 minutes) across the different land surface cover types (i.e., relict thermokarst lake, open moss, shrub, deciduous forest, sparse spruce, and dense spruce), together with four sub-sections of the cable sensor set in coil configurations (1.2 m high) and installed vertically half below and half above the ground to capture high-resolution vertical temperature profiles from the subsurface up to snowpack height at approximately 5 mm intervals. The total cable ran 2.3 km, within which about a 1.8 km section covered horizontal surface paths. Measurements were made from June 17, 2015, to September 19, 2016 (331 observation days). It provides “big data” for diurnal to seasonal variation analysis; however, it is also susceptive to

interruptions resulting from occasional power shutdowns, subsequent recovery failures, and partial failures or damage in the cable sensor caused by animals.

1. Background & Summary

Studies reveal that taiga regions, functioning as significant carbon sinks under the current eco-climatic conditions, exhibit considerable spatial variations (heterogeneity) in land cover, hosting dense and sparse forests, shrubs, grasses, open mosses, and bare ground. It is one of the challenges in quantifying the impacts of climate change in the boreal regions[1]. Located within the same area, each of these land cover types modulates energy, mass, and momentum exchange in boreal forests distinctively and in a nonlinear manner to influence geothermal flux, subsurface physical conditions, and microbial activity under seasonal changes differently[2-7] through their different characteristics in structural and functional features (e.g., the presence of and variation in different forms of canopy, aerodynamic and radiative characteristics, and phenology and snowpack) with the atmosphere[8,9]. Thence, sets of archived *in-situ* field measurements data, covering multiple observational points in a common area, can provide such empirical information as to quantify the spatiotemporal temperature patterns and variations, to constrain numerical eco-climatic models, and to assess the impacts of warming climate[10,11]in taiga regions.

Distributed temperature sensing (DTS) systems perform multi-sensor monitoring of an area using a fiber-optic cable configuration with high temporal and spatial resolutions. Developed in the 1980s and initially used in built-up environments[12-14] (e.g., industrial complexes and power plants), the technique was subsequently adapted for hydrological and geophysical research in natural environments[15-19]. This dataset updates the previous one that covered the portion of the measurement period from 2012 to 2014[20].

2. Location

The Poker Flat Research Range (65.12°N; 147.49°E, 210 meters above mean sea level) is a facility managed by the University of Alaska Fairbanks, located about 50 km northeast of Fairbanks in the interior of Alaska (Fig. 1). The area is in a discontinuous permafrost zone.

3. Methods

The DTS system measures temperatures along fiber-optic cable sensors using the Raman-scattering, optical time domain reflectometry techniques[12]. A laser pulse ejected from the equipment runs through the optical fiber (SiO_2) to excite the optical glass core and generates backscatter radiation at different frequencies (Figure 2d). The system records the Raman scattering to enable an analysis of the intensity ratios within the scatter spectrum (i.e., Stokes and anti-Stokes peaks) since the intensity at the latter peak is sensitive to the temperature of the medium, while that at the former is not. The travel time of the laser pulses derives the location of the temperature measured for the data (i.e., optical time domain reflectometry).

The DTS monitoring techniques continuously provide temperature data along the cable in spatially and temporally high resolution (e.g., half a meter and every 30 minutes, respectively. Figure 2a) under a wide range of ambient thermal conditions (from −40 °C in winter to 30 °C in summer). For the detailed equation form to retrieve the data, consult equation (1) in section 5.

The Loop1 study used a fiber-optic cable (multi-mode, GI50/125, dual-core; 3.4 mm, S2002A, manufactured by BRUGG, Switzerland), which is attached to the instrument (Figure 2b) at both ends to constitute the dual-mode observations. The cable sensor was initially installed in 2012 over 2.7 km long with a total of 2.0 km surface path (six horizontal sections), and 0.7 km for the five vertical sections coiled around PVC pipes[20] (Figure 2c). See Figures 2a and 3 for the horizontal section locations, from 1 to 5. However, both the end part of the horizontal section (ca. 300 m) and the fifth tube (total of ca. 100 m) were damaged by attacks from wild animals and discarded in 2015.

The software "DTS Configurator" that controls the behavior of the DTS measurements and produces the output data ("trace" files in text format) is developed and provided by the DTS system manufacturer (AP Sensing GmbH). The version used in 2016 was Ver.4.1.36, which ran on the Windows 7 operating system.

The explanations of the measurement methods are also provided[20] in terms of the physical principles, the equipment, and the fiber-optic cable sensors of the DTS measurements.

An observation tower was built in 2010 as part of a collaboration study (known as JICS) between the Japan Agency for Marine-Earth Science and Technology (JAMSTEC) and UAF's International Arctic Research Center (IARC)[21]. The following tower observations were used to calibrate and analyze the DTS measurements: air temperatures at 1.5m height, short-wave radiation measurements at 16m height (tower top), and snow depth using an ultrasonic sensor.

4. Data Records

The original output files (#3 below) can be read by general editors as it is in text (ASCII) format.

1. Attribution files.

(1) Temporal information (1 file)

A comma-separated-value text file with entities of [data number, year, month, day, hour, minute, second, and date] (Table 1).

The number of stored items is 17819. Here, the date denotes the elapsed date, with the fraction of a day, from January 1, 2015, beginning at noon, Alaska Standard Time.

Filename: TemporalData_Loop1_2015_2016.csv.

(2) Locational information (1 file)

A comma-separated-value text file with entities of [data number, longitude, latitude, section number, section information, observation number in the section] (Table 2, Figure 3).

The number of stored items is 8870.

Filename: SectionData_Loop1_2015_2016.csv.

2. Quality-controlled temperature data file (1 file)

An unformatted binary (4-byte float) data file only of the temperature [°C] data, extracted from the quality-controlled output files (#3 below).

It has the (location, time) dimension as described above in #1, and is in the size of 632,218,120 bytes (= 8870 x 17819 x 4). See Figure 4 for coverage of the successful, quality-controlled data in time and space.

Filename: Loop1_temperature_2015_2016.dat

3. Original output files (324 files)

Original trace files that were the target of the quality control (i.e., checking for no missing or inappropriate values) as described in 5. Technical Validation, 3).

A trace file is produced by the "DTS Configurator" software in text format ("dtsout1-YYYYMMDD00N000.tra"), where YYYY, MM, and DD are the year, month, and day of the data production, and N is the order of products in the same day. The first 117 lines are header information on the measurement settings. Each observation output starts with "[Trace.xxx]," where xxx denotes the number of consecutive measurements, and ends with temporal information when the output was produced.

Each line of output has the following entries separated by a semicolon: "Number; distance [meter]; temperature [°C]; original DTS signal [-]; loss of signal [dB]"

Data example:

```
[Trace.8967]
0;0;10.0109920501709;-8.47090148925781;-0.352133858203888
1;0.5;7.30609560012817;-8.54311180114746;-0.332597585519155
2;1;4.21356058120728;-8.62734889984131;-0.334414551655451
3;1.5;2.62092041969299;-8.67144870758057;-0.335013677676519
(omission)
10464;5232;3.28256893157959;-8.65306758880615;-8.3079355875651
10465;5232.5;4.9467248916626;-8.60721397399902;-8.33420785268148
10466;5233;7.42107248306274;-8.54001426696777;-8.41131579081218
```

(omission)

Date.Year;2016

Date.Month;1

Date.Day;5

Time.Hour;0

Time.Minute;23

Time.Second;6

5. Technical Validation

We have taken the following measures to assure the technical quality of the measurements and the compiled data: 1) calibration of the measured temperature of the cable sensor, 2) comparison of the DTS measurement with another observation (namely, the JICS tower observations[21]. cf. Figure 5[20]), and 3) removal of the failed observations due to breaks or inappropriate fusion of the cables.

1) Calibration of the measured temperature of the cable sensor

Temperature measurement of the DTS, T in the unit of [K], at the distance x [m] at the time t [s] can be obtained by the following equation (see equation (20.2)[22]).

$$T(x,t) = \frac{\gamma}{\ln\left(\frac{P_S(x,t)}{P_{AS}(x,t)}\right) + C(t) + \Delta\alpha x}, \quad (1)$$

where γ [K] is a constant value for temperature calibration representing the system-specific shift in energy associated with the Raman backscatter, P_S and P_{AS} stand for the respective strength of the Stokes and Anti-Stokes signal from the Raman backscatter, $C(t)$ is a dimensionless parameter representing the instrument characteristics, and $\Delta\alpha$ denotes a constant attenuation ratio along the cable sensor. For the physical calibration for a dual-ended measurement mode, in which the cable is attached to the DTS instrument at both ends, we kept a section of the cable (*ca*. a length of 10 meters or longer) at the freezing temperature (0°C) environment to determine the value γ, and the attenuation ratio is determined by the instrument automatically. (N.B., for a single-ended mode where the cable is attached to the instrument at one end of the cable, requires either two different sections for temperature calibration or the same section at two different temperatures.)

2) Comparison of the DTS measurement with another observation

The DTS measurements taken at the 30-minute interval were compared to the JICS tower observations and analyzed for diurnal and seasonal changes (cf. Section 3[21]).

3) Removal of the failed observations due to breaks or inappropriate fusion of the cables

The DTS measurements are disrupted when the cable sensor is damaged permanently by cuts or breaks of the cable, or occasionally or permanently by fusion failures at the conjunction of the cables. Those disrupted measurements are detected by the discontinuity of the signal loss level. We checked through the datasets to discard such measurements that showed such discontinuity as shown in Figure 6. The observations were also interrupted by occasional power outages, leading to failures of observations for the entire section. Despite auto-recovery of the measurements after the outages, intervals of successful observations may be longer than scheduled (i.e., 30 minutes).

6. Usage Notes

It should be noted that, as a nature of time domain reflectometry, each measured value at a point does not necessarily indicate the point-wise temperature at the corresponding point, but rather averaged temperature along the intervals that contain the point.

7. Competing interests

There are no competing interests in this study.

8. Figures

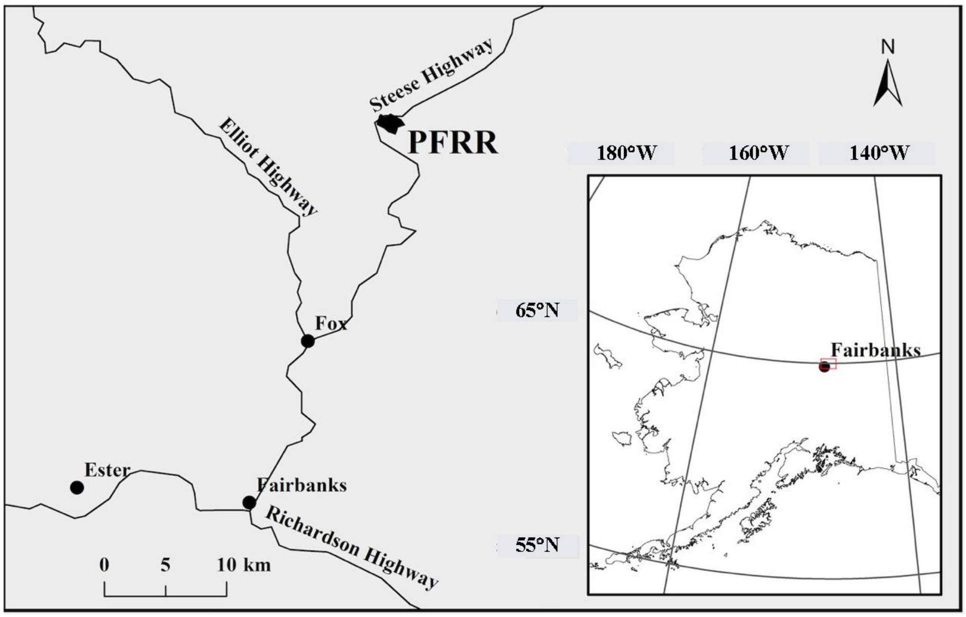

Figure 1. Location of the DTS system installed at the Poker Flat Research Range (PFRR; University of Alaska Fairbanks). [Reproduced from Saito *et al.* (2018)[20]]

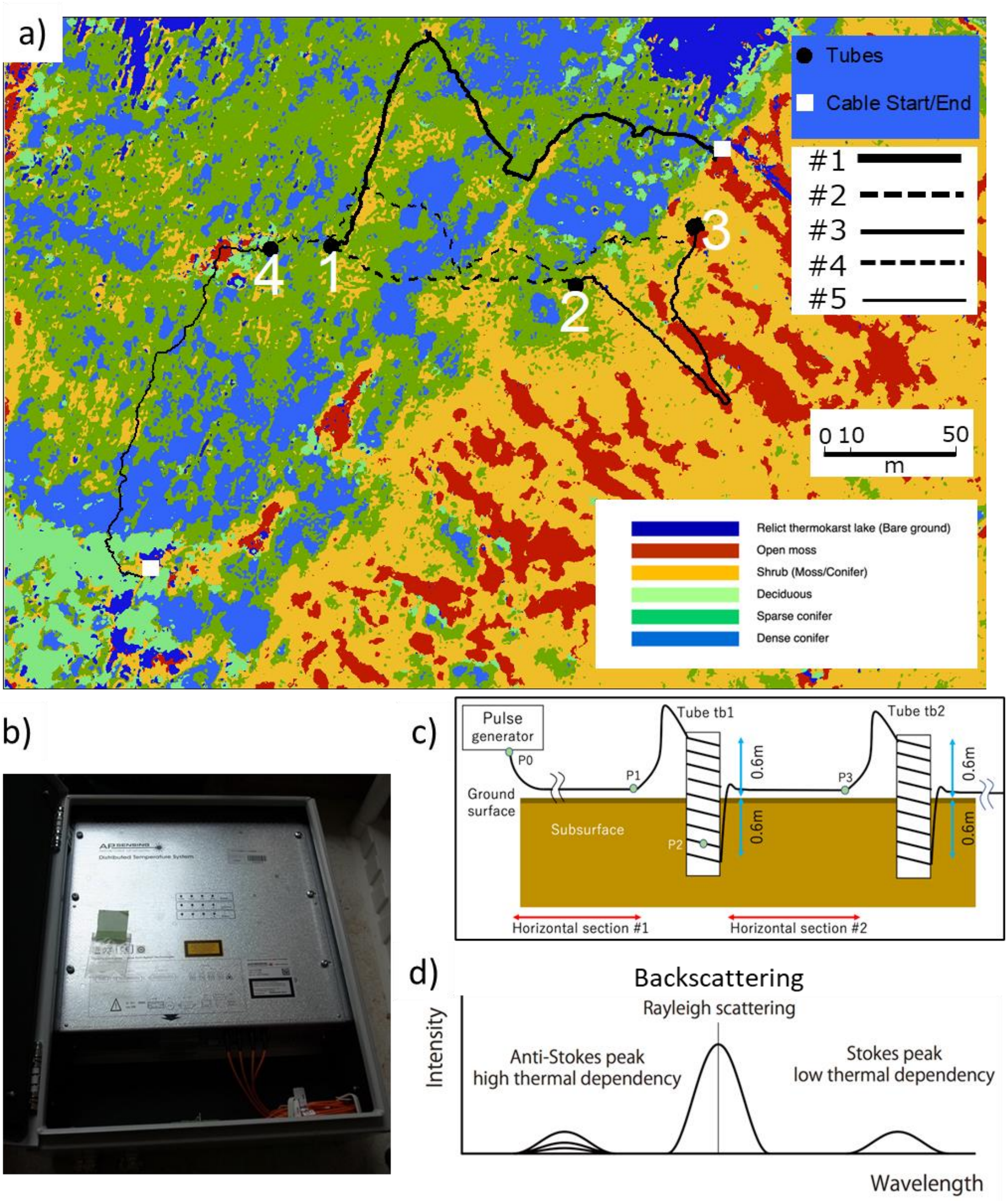

Figure 2. a) Installation information of the Loop1 fiber-optic cable in 2016 at Poker Flat Research Range. Horizontal sections of the cable sensor are delineated by different lines. Numbers in white denote the tube sections. Colors show the surface cover types. b) Photo of the DTS equipment (AP SENSING N4386B). c) Schematic diagram of fiber-optic cable deployment for the horizontal and tube (vertical) sections. d) Explanatory diagram of the Raman backscattering. See text and equation (1) in section 5 for the methodology to derive temperature information from the backscattering.

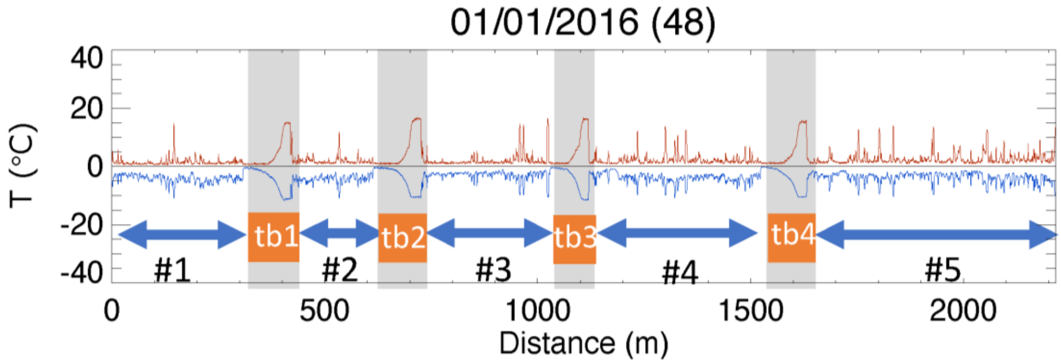

Figure 3. Daily summary of the DTS observations on January 1, 2016. The daily average is shown in blue, and the range is in red. Sectioning of the cable for inter-tubes (#1 to #5) and tubes (tb1 to tb4) are also shown. The figure in round parentheses in the title denotes the number of successful observations on the day.

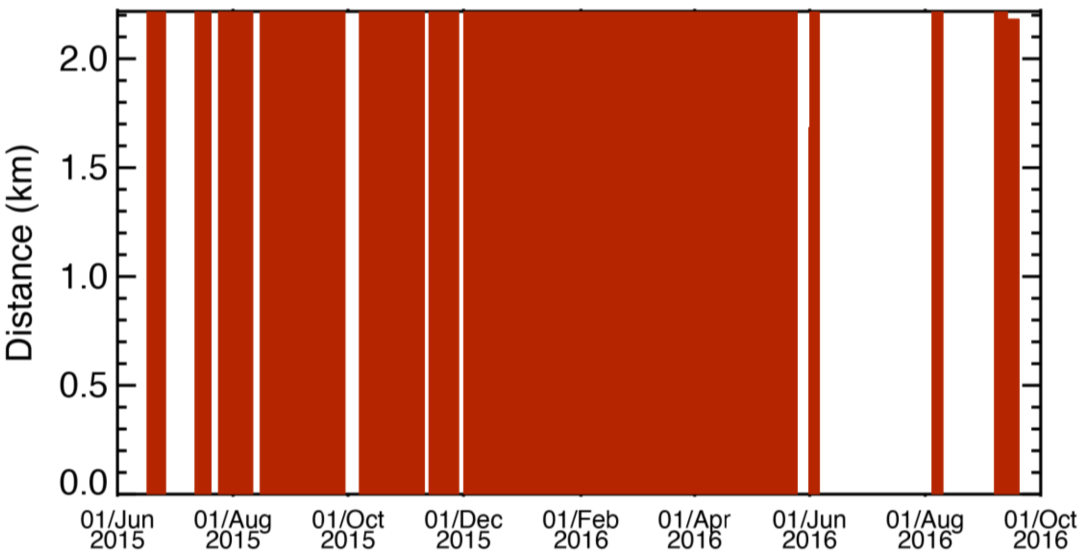

Figure 4. Dates and locations of the successful observations by Distributed Temperature Sensing (DTS) system from 2015 to 2016. Successful observations are shown in red.

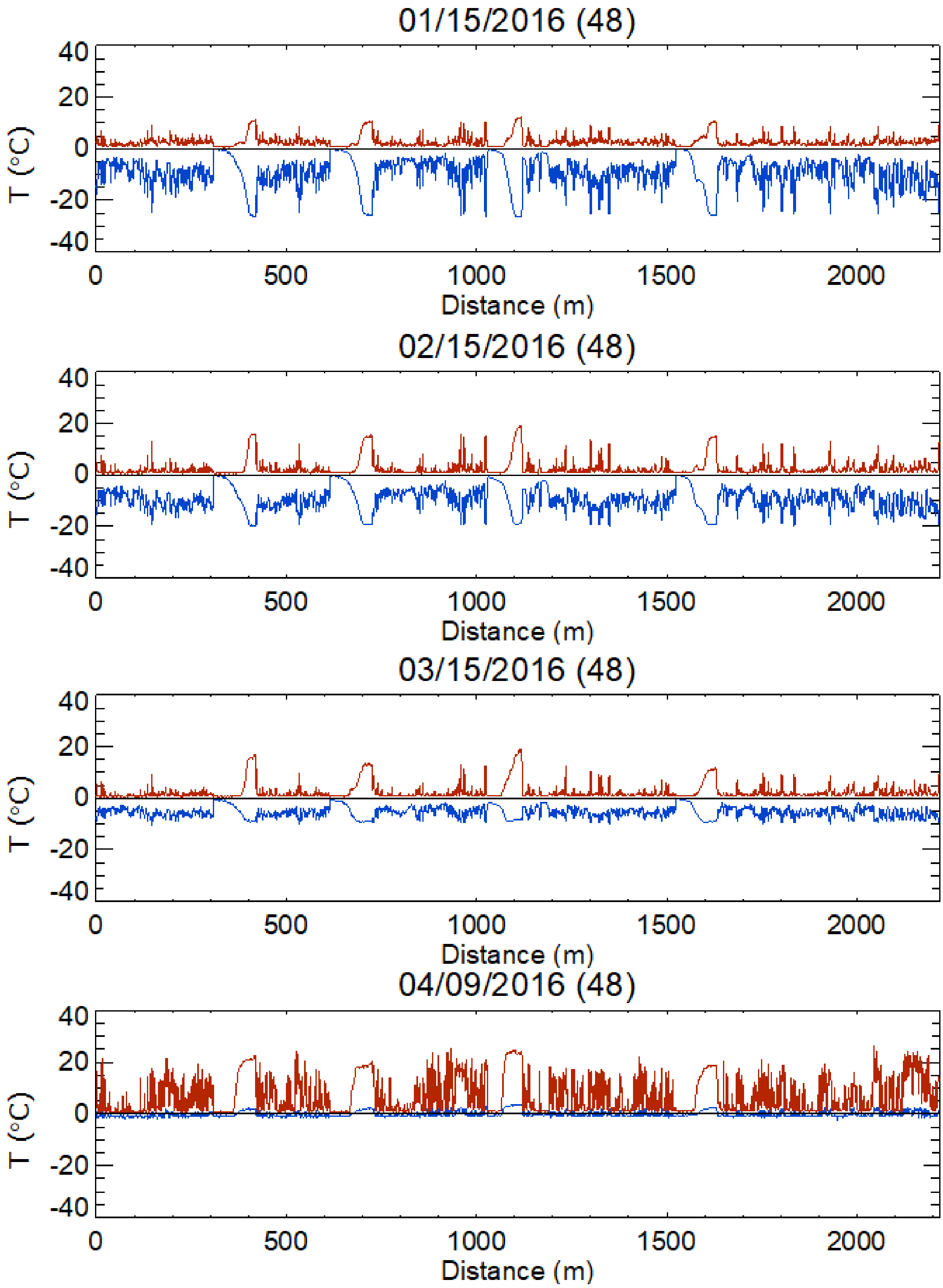

Figure 5. Examples of Loop1 daily summary (average in blue, and range in red) in 2016. The figure in round parentheses in the title denotes the number of observations on the day.

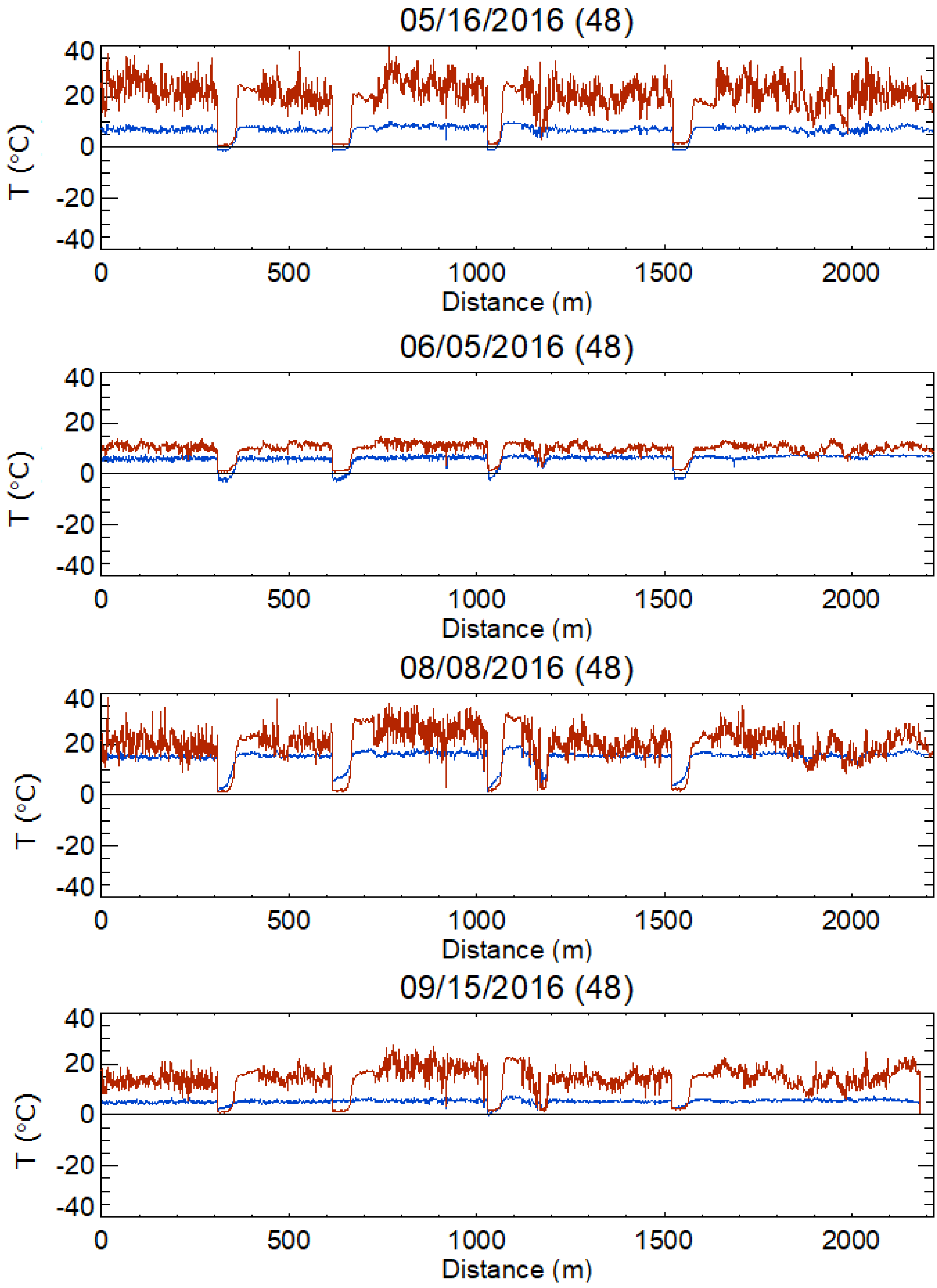

Figure 5. (Continued)

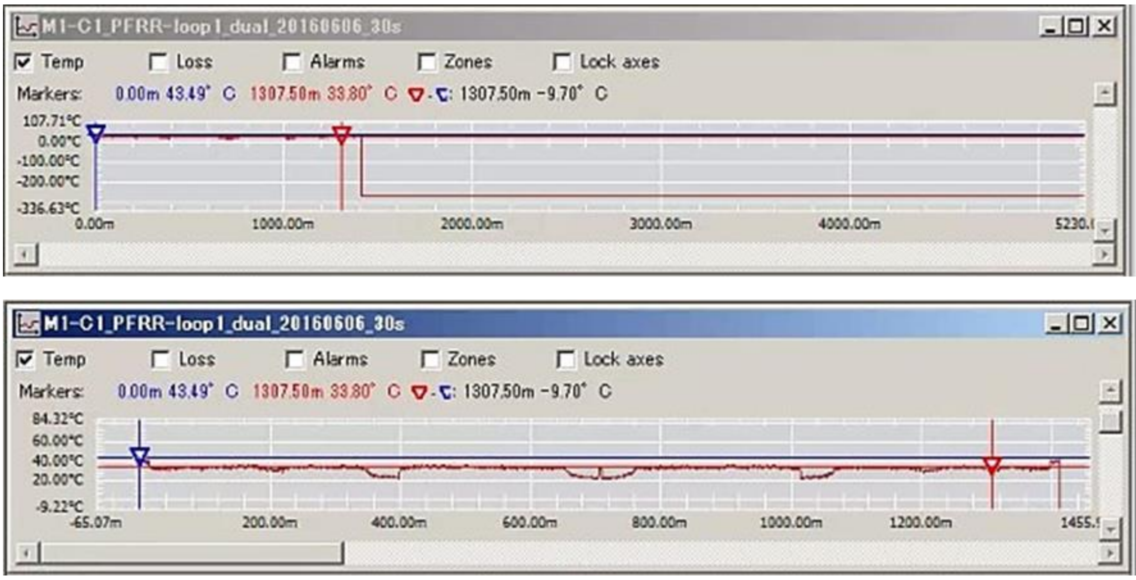

Figure 6. Examples of incomplete observation due to cable failure around the 1410-meter point on June 20, 2016. After the failure (break of the cable) the observed values show -273.15℃, which indicates missing values. (Upper) observed results for the entire span (from 0 to 5700 m). (Lower) Exert for the earlier observation section (from 0 to 1455 m).

9. Tables

Table 1. The data structure of the temporal information file.

	A	B	C	D	E	F	G	H
1	Temporal Information							
2	#	Year	Month	Day	Hour	Minute	Second	Date
3	0	2015	6	17	0	22	37	166.515706
4	1	2015	6	17	0	52	37	166.536539
5	2	2015	6	17	1	22	37	166.557373
6	3	2015	6	17	1	52	37	166.578206
7	4	2015	6	17	2	22	37	166.599039
8	5	2015	6	17	2	52	37	166.619873
9	6	2015	6	17	3	22	37	166.640706
10	7	2015	6	17	3	52	37	166.661539
11	8	2015	6	17	4	22	37	166.682373
12	9	2015	6	17	4	52	37	166.703206
13	10	2015	6	17	5	22	37	166.724039
14	11	2015	6	17	5	52	37	166.744873
15	12	2015	6	17	6	22	37	166.765706
16	13	2015	6	17	6	52	37	166.786539
17	14	2015	6	17	7	22	36	166.807361
18	15	2015	6	17	7	52	36	166.828194
19	16	2015	6	17	8	22	36	166.849028
20	17	2015	6	17	8	52	36	166.869861
21	18	2015	6	17	9	22	36	166.890694
22	19	2015	6	17	9	52	36	166.911528

Table 2. The data structure of the locational information file.

	A	B	C	D	E	F	G
1	Section Information: f1(Start=>Tube1, forward), tb1(Tube1, forward),						
2	f2(Tube1 = > Tube2, forward), tb2(Tube2, forward), ..., f5(Tube4 = > End, forward),						
3	r5(End = > Tube4, backward), rb4(Tube4, backward), f4(Tube4 = > Tube3, backward), ...						
4	#	Longitude	Latitude	Section #	Section Info	Obs # in section	
5	0	-147.48987	65.1240631	1	f1	1	
6	1	-147.48987	65.1240548	1	f1	2	
7	2	-147.48986	65.1240503	1	f1	3	
8	3	-147.48986	65.1240477	1	f1	4	
9	4	-147.48986	65.1240482	1	f1	5	
10	5	-147.48986	65.1240507	1	f1	6	
11	6	-147.48986	65.1240552	1	f1	7	
12	7	-147.48986	65.124059	1	f1	8	
13	8	-147.48985	65.1240618	1	f1	9	
14	9	-147.48985	65.1240658	1	f1	10	
15	10	-147.48985	65.1240701	1	f1	11	

Author contributions

K. Saito initiated, designed, and supervised the entire project; procured the sets of equipment, negotiated the use of PFRR, and led the deployment of the cable sensor, the calibrations, programming, and measurements by the DTS system. G. Iwahana and R. Busey contributed installation of the DTS equipment. GI, H. Nagano, and H. Ikawa contributed to maintaining DTS measurement. GI conducted land cover classification for the site and generated figures of geographical information. RB supervised the technical aspects of the project. All the authors contributed to the final manuscript with input, suggestions, and editing.

Acknowledgements

This project was conducted as a part of the JAMSTEC (Japan Agency for Marine-Earth Science and Technology) and IARC (International Arctic Research Center, University of Alaska, Fairbanks) collaboration study, and in part supported by the “Integrated Research Program for Advancing Climate Models (TOUGOU Program, JPMXD0717935715)”, the Arctic Challenge for Sustainability (ArCS, JPMXD1300000000), and the Arctic Challenge for Sustainability II (ArCS II, JPMXD1420318865). KS is grateful to Drs. Masao Fukasawa, Hide Sakaguchi, Akira Noda, and Michio Kawamiya for their support in initiating and conducting the DTS project. The authors are grateful to Dr. Kathe Rich, and Mr. Robert Valdez for their cooperation and facilitation in investigating at the PFRR site.

References

1. Hinzman, L. D. et al. Evidence and Implications of Recent Climate Change in Northern Alaska and Other Arctic Regions. Climate Change. 2005, 72, p. 251–298. https://doi.org/10.1007/s10584-005-5352-2.
2. Euskirchen, E. S. et al. Importance of recent shifts in soil thermal dynamics on growing season length, productivity, and carbon sequestration in terrestrial high-latitude ecosystems. Glob. Change Biol. 2006, 12 (4), p. 731–750. https://doi.org/10.1111/j.1365-2486.2006.01113.x.
3. Essery, R. et al. SNOWMIP2: An Evaluation of Forest Snow Process Simulations. B. Am. Meteorol. Soc. 2009, 90, p. 1120–1135. https://doi.org/10.1175/2009BAMS2629.1.
4. Rutter, N. et al. Evaluation of forest snow processes models (SnowMIP2), J. Geophys. Res. 2009, 114, D06111. https://doi.org/10.1029/2008JD011063.
5. Kasurinen, V. et al. Latent heat exchange in the boreal and arctic biomes. Glob. Change Biol. 2014, 20 (11), p. 3439–3456. https://doi.org/10.1111/gcb.12640.
6. Ikawa, H. et al. Understory CO_2, sensible heat, and latent heat fluxes in a black spruce forest in interior Alaska. Agr. Forest Meteorol. 2015, 214–215, p. 80–90. https://doi.org/10.1016/j.agrformet.2015.08.247.
7. Purdy, A. J., Fisher, J. B., Goulden, M. L., and Famiglietti, J. S. Ground heat flux: An analytical review of 6 models evaluated at 88 sites and globally. J. Geophys. Res. Biogeosci. 2016, 121 (12), p. 3045–3059. https://doi.org/10.1002/2016JG003591.
8. Vrese, P., Schulz, J.-P., and Hagemann, S. On the Representation of Heterogeneity in Land-Surface–Atmosphere Coupling. Bound.-Lay. Meteorol. 2016, 160, p. 157–183. https://doi.org/10.1007/s10546-016-0133-1.
9. Sellers, P. Modeling and observing land-surface-atmosphere interactions on large scales. Surv. Geophys. 1991, 12, p. 85–114. https://doi.org/10.1007/BF01903413.
10. Beer, C., Lucht, W., Gerten, D., Thonicke, K., and Schmullius, C. Effects of soil freezing and thawing on vegetation carbon density in Siberia: A modeling analysis with the Lund–Potsdam–Jena Dynamic Global Vegetation Model (LPJ-DGVM). Global Biogeochem. Cy. 2007, 21 (1), GB1012. https://doi.org/10.1029/2006GB002760.
11. Sato, H., Kobayashi, H., Iwahana, G., and Ohta, T. Endurance of larch forest ecosystems in eastern Siberia under warming trends. Ecol. Evol. 2016, 6 (16), p. 5690–5704. https://doi.org/10.1002/ece3.2285.
12. Dakin, J. P., Pratt, D. J., Bibby, G. W., and Ross, J. N. Distributed optical fibre Raman temperature sensor using a semiconductor light source and detector. Electron. Lett. 1985, 21 (13), p. 569–570. https://doi.org/10.1049/el:19850402.
13. Dyer, S. D., Tanner, M. G., Baek, B., Hadfield, R. H., and Nam, S. W. Analysis of a distributed fiber-optic temperature sensor using single-photon detectors. Opt. Express. 2012, 20 (4), p. 3456–3466. https://doi.org/10.1364/OE.20.003456.
14. Soto, M. A., Ramírez, J. A., and Thévenaz, L. Intensifying the response of distributed optical fibre

sensors using 2D and 3D image restoration. Nat. Commun. 2016, 7, 10870. https://doi.org/10.1038/ncomms10870.

15. Selker, J., van de Giesen, N., Westhoff, M., Luxemburg, W., and Parlange, M. B. Fiber optics opens window on stream dynamics. Geophys. Res. Lett. 2006a, 33 (24), L24401. https://doi.org/10.1029/2006GL027979.
16. Selker, J. S. et al. Distributed fiber-optic temperature sensing for hydrologic systems. Water Resour. Res. 2006b, 42 (12), W12202. https://doi.org/10.1029/2006WR005326.
17. Tyler, S. W. et al. Environmental temperature sensing using Raman spectra DTS fiber-optic methods. Water Resour. Res. 2009, 45 (4), W00D23, https://doi.org/10.1029/2008WR007052.
18. Thomas, C. K. et al. High-Resolution Fibre-Optic Temperature Sensing: A New Tool to Study the Two-Dimensional Structure of Atmospheric Surface-Layer Flow. Bound.-Layer Meteorol. 2012, 142, p. 177–192. https://doi.org/10.1007/s10546-011-9672-7.
19. Lutz, J. A., Martin, K. A., and Lundquist, J. D. Using Fiber-Optic Distributed Temperature Sensing to Measure Ground Surface Temperature in Thinned and Unthinned Forests. Northwest Sci. 2012, 86 (2), p. 108–121. https://doi.org/10.3955/046.086.0203.
20. Saito, K., Iwahana, G., Ikawa, H., Nagano, H., and Busey, R. C. Links between annual surface temperature variation and land cover heterogeneity for a boreal forest as characterized by continuous, fibre-optic DTS monitoring. Geosci. Instrum. Method. Data Syst. 2018, 7 (3), p. 223–234. https://doi.org/10.5194/gi-7-223-2018.
21. Nakai, T. et al. Characteristics of evapotranspiration from a permafrost black spruce forest in interior Alaska. Polar Sci. 2013, 7 (2), p. 136–148. https://doi.org/10.1016/j.polar.2013.03.003.
22. Thomas, C. K. and Selker J. Optical Fiber-Based Distributed Sensing Methods. Foken, T. (ed.) Springer Handbook of Atmospheric Measurements. Springer Handbooks. Springer, Cham. 2021, p. 609–631. https://doi.org/10.1007/978-3-030-52171-4_20.

Data Citations

Saito, K., Iwahana, G., Ikawa, H., Nagano, H., and Busey, R. Spatio-temporally continuous temperature monitoring using optical fibers (Loop1) in the internal forest areas at Alaska in 2016. 3.00, Japan, Arctic Data archive System (ADS), 2023. https://doi.org/10.17592/001.2019062501.